TEKST NR 314 1996

Feedback Regulation of Mammalian Cardiovascular System

By
Johnny T. Ottesen

TEKSTER fra
IMFUFA ROSKILDE UNIVERSITETSCENTER
INSTITUT FOR STUDIET AF MATEMATIK OG FYSIK SAMT DERES
FUNKTIONER I UNDERVISNING, FORSKNING OG ANVENDELSER

IMFUFA, Roskilde Universitetscenter, Postboks 260, 4000 Roskilde, Denmark

Feedback Regulation of Mammalian Cardiovascular System
by: Johnny T. Ottesen

IMFUFA-tekst nr. 314/96 32 pages ISSN 0106-6242

Abstract:

The cardiovascular system is considered. A Direct modelling of the non-linear baroreflex-feedback mechanism, including time-delay, is developed based on physiological theory and empirical facts. The feedback model is then evaluated on an expanded, but simple, Windkessel model of the cardiovascular system. The stability of the entire model is analyzed and the effect of the value of the time-delay is investigated and discussed. The time-delay may cause oscillations. A finite number of stability switches may occur dependent on the value of the time-delay. The location of these stability switches turn out to be sensitive to the value of the parameters in the model. We suggest a simple experiment to determinate whether or not the time-delay is responsible for the 10 second Mayer waves. Data from an ergometer bicycle test is used for evaluation of the model.

Feedback Regulation of Mammalian Cardiovascular System

JOHNNY T. OTTESEN
IMFUFA, Roskilde University
Postbox 260, DK-4000 Roskilde
E-mail: Johnny@mmf.ruc.dk

30th April 1996

Abstract

The cardiovascular system is considered. A Direct modelling of the non-linear baroreflex-feedback mechanism, including time-delay, is developed based on physiological theory and empirical facts. The feedback model is then evaluated on an expanded, but simple, Windkessel model of the cardiovascular system. The stability of the entire model is analyzed and the effect of the value of the time-delay is investigated and discussed. The time-delay may cause oscillations. A finite number of stability switches may occur dependent on the value of the time-delay. The location of these stability switches turn out to be sensitive to the value of the parameters in the model. We suggest a simple experiment to determinate whether or not the time-delay is responsible for the 10 second Mayer waves. Data from an ergometer bicycle test is used for evaluation of the model.

1 Introduction

We consider the systemic part of the cardiovascular system, consisting of the left ventricle, the arteries, the capillaries, the veins, and the right ventricle, together with the baroreflex-feedback mechanism.

The mathematical modeling of this system, without feedback, can be approached in several ways. One may derive partial differential equations,

describing the blood as a Newtonian fluid, for this approach see for example Sir Lighthill (1975), Peskin (1976), Pedley (1980), Berger (1993) and Olufsen & Ottesen (1995). Rather than this, we make the model as rough as possible, focusing on simple and well-established physical principles, and make as many simplifying physical assumptions as possible. Hereby, a system of ordinary differential equations with only a few variables is obtained, for this approach see Warner (1958), Grodins (1959), Warner & Cox (1962), Warner (1962), Grodins (1963), Milhorn (1966), Taylor (1978), Noordergraaf (1978), Usino (1995) and Cavalcanti et al. (1995). This part of the modeling is based on theoretical physics (section 2-5). Having a model of the uncontrolled cardiovascular system (that is, excluding feedback mechanisms) we extend the model, by adding an explicit modelling of the chronotropic and inotropic effect of the baroreflex-feedback mechanism. There have been several attempt to model the accumulated effect of the baroreflex-feedback mechanism as a regulator by standard methods known from control theory. Noldus (1976) used optimal control based on a principle of minimal energy consumption whereas Ono et al. (1982) and Kappel & Peer (1993) used optimal control based on a priciple of minimal deviation from a set-point. None of these are based on well-established physiological knowledge. Rideout (1991) and Tham (1988) used principles from linear control theory, even though the feedback is not linear. We prefer to model the feedback mechanism directly. Our approach is based on well-established physiological theory and empirical facts, i.e. on physiological knowledge (section 6-7). This feedback mechanism introduces some non-linearity in the model and includes time-delay. Special attention is paid to the effect of the time-delay.

When such a feedback model is produced, we apply methods from non-linear analysis, which are very useful in this connection. The various possible scenarios, coursed by different values of the time-delay, are discussed together with a possible relation to the 10 second Mayer waves (section 8). Moreover an ergometer bicycle test is simulated and compared to real data (section 9). However, it is not possible to solve all equations analytically, and we therefore include numerical considerations.

Finally a discussion and an outlook is given (section 10) and the nominal values of the parameter used is listed (appendix).

One may model the pulmonary part of the cardiovascular system in a similar way as the systemic part. A model of the entire cardiovascular system does not separate into two uncoupled submodels, even when pressure independent stroke volumes are assumed, because of conservation of the total blood volume. However, such a model includes a submodel of the systemic part of the cardiovascular system, which is independent of the rest of the system.

Therefore, an analysis of the systemic part of the cardiovascular system is sufficient for our considerations.

Finally gratitude is given to Professor F. Kappel and O. Peer for letting us use their data, obtained from ergometer bicycle tests, which we use for validation of the model.

2 Physical Model of the Uncontrolled Cardiovascular System

First we consider the systemic part of the cardiovascular system, consisting of the left ventricle, the arteries, the capillaries, the veins, and the right ventricle, without feedback mechanisms. Later we add a model of the baroreflex-feedback mechanism.

Since our goal is to analyze the baroreflex-feedback mechanism, the model of the uncontrolled system must be as simple as possible, yet still has to catch certain principal characteristics of the system. Hereby we can handle the feedback model and understand the basic mechanism of the real system being modeled.

We include the left ventricle in the model only to describe the inflow to the aorta. Therefore, we describe it simply as a source term, i.e. the inflow is given by a function of time. This function is chosen to agree with measurements and depends on heart rate and contractility (or stroke volume).

The arteries are considered as a compartment characterized by a compliance. The pressure in the arterial compartment is determined by the difference between inflow to and outflow from the compartment, see figure 1.

From the arteries there is an outflow, through the capillaries, to the venous part. Since the major drop in pressure occurs over the capillaries, Guyton (1981), they are characterized by a resistance to the flow. Hence, the flow through the capillaries is determined by the difference in pressure between the arterial and the venous part.

Analogous to the arteries, the veins are considered as a compartment characterized by another compliance.

The flow out of the veins is into the right ventricle, ignoring the right atrium. The ventricle is simply described as a sink, characterized by a resistance to the flow out.

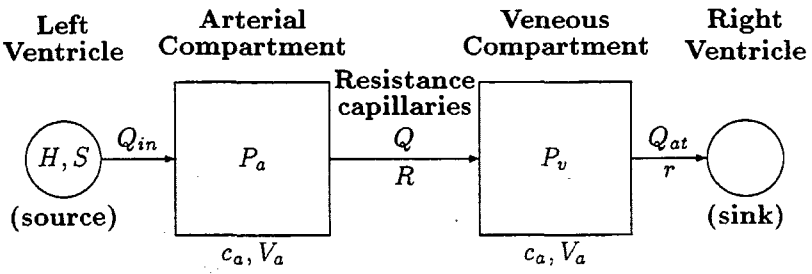

Figure 1: A lumped uncontrolled model of the cardiovascular system.

The above idealizations, lumping the systems into compartments, as shown on figure 1, are rough in some respects, e.g. one loose information about spatial properties. However, it turns out that the model is adequate for the following analysis of the baroreflex-feedback mechanism.

3 Mathematical Model of the Uncontrolled Cardiovascular System

Now we turn to the mathematification of the physical model presented in section 2. In the following considerations the blood is treated as an incompressible Newtonian fluid. We further ignore the fluid exchange between the blood circulation and the interstitial fluid space.

The outflow, Q_{in}, from the left ventricle may be described in an ad-hoc manner, just to agree with measurements, as follows

$$Q_{\text{in}}(t) = \begin{cases} 0 & \text{, for } t > t_s \text{ modulo } T \\ S \cdot t_s^{-m} \sin(\pi(1 - \frac{t}{t_s})^3) & \text{, for } t \leq t_s \text{ modulo } T \end{cases}$$

Where T is the heart cycle, S the contractility of the heart, t_s the duration of systole and m describe how the stroke volume depends of the duration of systole. For $m = 1$ there is no dependence, for $m < 1$ the stroke volume is decreasing with t_s, which describe the usual physiological situation, in fact, $V_{\text{str}} = S \cdot \int_0^T Q_{\text{in}}(t)dt \propto S \cdot t_s^{1-m}$. The fact that Q_{in}, and then V_{str}, is linear in the contractility, S, follows from a detailed analysis of the ventricle. To relate t_s and T one may use the empirical law, $t_s = \kappa\sqrt{T}$, where $\kappa \in [0.3, 0.5]$ when the time units is second, Kappel & Peer (1993). A detailed modelling of the ventricle suggest that $V_{\text{str}} \propto S \cdot t_s$, i.e. $m = 0$.

We use the above description of the left ventricle as a source to avoid a complex model of the heart and to reduce the number of state variables.

Conservation of mass suggest that the time-derivative of the arterial volume $\dot{V}_a$ is given by

$$\dot{V}_a(t) = Q_{\text{in}}(t) - Q(t)$$

where Q is the outflow from the arteries (see figure 1).

To obtain a state equation relating arterial spatial mean pressure, P_a, and volume, V_a, we choose the mathematical most simple one which agree pretty well with measurements.

$$P_a = \frac{1}{c_a} V_a$$

where c_a is a constant, describing the compliance of the arterial system. This constitutive equation is commonly used in the literature. Eliminating the volume we get

$$\dot{P}_a(t) = \frac{1}{c_a}(Q_{\text{in}}(t) - Q(t))$$

Quite analogue the venous part is modeled, relating venous spatial pressure, P_v, and volume, V_v, giving the equation

$$\dot{P}_v(t) = \frac{1}{c_v}(Q(t) - Q_{\text{out}}(t))$$

where c_v is a constant, describing the compliance of the venous system, and Q_{out} is the outflow from the veins. However, in the venous case, the constitutive equation $P_v = \frac{1}{c_v} V_v$ do not agree as well with measurements as in the arterial case. Another choice could be $P_v = \frac{1}{c_v} V_v^n$, with $n > 1$. This choice agree better with measurements for suitable value of n, Warner & Cox (1962). Nevertheless, we prefer the original choice for purely simplifying reasons. For a further discussion of the venous part we refer to Noordergraaf (1978).

We use a lumped parameter model to describe the flow, Q, through the capillaries. Conservation of momentum, assuming no friction, may be described by the equation

$$\partial_t \int_V \rho u(t) dV = \int_A p(t) dA$$

where ρ is the density of blood, u the time-dependent velocity-field, p the time-dependent pressure-field, A the cross-section area, and V the volume. However, due to friction there is a resistance to flow and then a loss of momentum, which is assumed to bee proportional to the flow, corresponding to

laminar flow, and characterized by a resistance R. Then the above conservation equation has to be modified as follows

$$\partial_t \int_V \rho u(t) dV = \int_A p(t) dA - RAQ(t)$$

Then

$$\rho L_0 A \dot{Q}(t) = (P_a(t) - P_v(t))A - RAQ(t)$$

where the length of the compartment L_0 is related to the cross-section area A and the volume V as $A \cdot L_0 = V$. Furthermore, Q is the average of the flow, $Q(t) = \frac{1}{A}\int_A u(t) dA$, in the length direction. Then, with $L = \rho L_0$, describing the inertia of the blood, we get the well-known equation (see Noordergraaf (1978))

$$\dot{Q}(t) = -\frac{R}{L}Q(t) + \frac{1}{L}(P_a(t) - P_v(t))$$

Finally, we describe the outflow from the veins to the right ventricle during diastole as a sink, characterized by a resistance, r, to the flow out. In analogy with the capillary case we get

$$\dot{Q}_{\text{out}}(t) = -\frac{r}{l}Q_{\text{out}}(t) + \frac{1}{l}(P_v(t) - 0)$$

where l characterize the inertia of the blood, in analogy with L above.

Then the complete model of the pulsatile uncontrolled cardiovascular system is given by the inflow function

$$Q_{\text{in}}(t) = \begin{cases} 0 & \text{, for } t > t_s \bmod T \\ S \cdot t_s^{-m} \sin(\pi(1 - \frac{t}{t_s})^3) & \text{, for } t \leq t_s \bmod T \end{cases} \tag{1}$$

where $t_s = \kappa\sqrt{T}$ and the following four differential equations

$$\dot{P}_a(t) = \frac{1}{c_a}(Q_{\text{in}}(t) - Q(t)) \tag{2}$$

$$\dot{Q}(t) = -\frac{R}{L}Q(t) + \frac{1}{L}(P_a(t) - P_v(t)) \tag{3}$$

$$\dot{P}_v(t) = \frac{1}{c_v}(Q(t) - Q_{\text{out}}(t)) \tag{4}$$

$$\dot{Q}_{\text{out}}(t) = -\frac{r}{l}Q_{\text{out}}(t) + \frac{1}{l}P_v(t), \text{ for } t \geq t_s \bmod T \tag{5}$$

$$Q_{\text{out}}(t) = 0, \text{ for } t < t_s \bmod T \tag{6}$$

We emphasize that the pulmonary part of the cardiovascular system may be described in a complete analogue manner. Then a model of the entire

cardiovascular system is obtained if we, for each ventricle, remodel the sink term such that it equal the source term, when integrated over a cycle. Furthermore, we have to include conservation of the total blood volume.

Before studying the pulsatile model further, we discuss the non-pulsatile model, which arrive from the pulsatile one by averaging over a heart cycle. This is partly motivated by the fact, that it is the average arterial pressure which, through the baroreflex-feedback mechanism, steer the change in heart rate and contractility (or stroke volume). We return to these feedback mechanisms in section 7.

4 Mathematical Model of the Non-pulsatile System

The non-pulsatile model is obtained by beat-to-beat averring of the pulsatile model, giving in equations (1)–(6), i.e. averaging over a cycle. Hereby one obtain a system of equations as follows

$$Q_{\text{in}}(t) = St_s^{-m+1}\frac{1}{T}\int_0^{\pi^{1/3}} \sin(x^3)dx \equiv HV_{\text{str}} \tag{7}$$

$$\dot{P}_a(t) = \frac{1}{c_a}(Q_{\text{in}}(t) - Q(t)) \tag{8}$$

$$Q(t) = \frac{1}{R}(P_a(t) - P_v(t)) \tag{9}$$

$$\dot{P}_v(t) = \frac{1}{c_v}(Q(t) - Q_{\text{out}}(t)) \tag{10}$$

$$Q_{\text{out}}(t) = \frac{1}{r}P_v(t) \tag{11}$$

where $H = \frac{1}{T}$ is the heart rate, V_{str} is the stroke volume, and all variables are now average values over one cycle. The reason for equation (10) and (12) is that the accelerations are small and that $\frac{1}{L}$ and $\frac{1}{l}$ both are large (a stringent argument may be found in the theory of perturbations of differential equations, see Murdock (1991).) Note that the system (7)–(11) may be thought of as depending on the heart rate and the stroke volume, rather than on Q_{in} explicitly. Notice that the contractility doesn't appear explicitly, but is integrated in the stroke volume. Therefore we think of heart rate and stroke volume as our control variable and the corresponding feedback mechanism will be called the chronotropic effect and the inotropic effect, respectively.

Hence, the differential equations describing the mathematical model of the non-pulsatile system becomes

$$\dot{P}_a(t) = \frac{1}{c_a} HV_{\text{str}} - \frac{1}{c_a R}(P_a(t) - P_v(t)) \tag{12}$$

$$\dot{P}_v(t) = \frac{1}{c_v R} P_a(t) - (\frac{1}{c_v R} + \frac{1}{c_v r}) P_v(t) \tag{13}$$

Notice that this is almost the equations first derived by Grodins (1959), except for the outflow part. In the next section we are going to analyze this two-dimensional dynamical system.

5 Analysis of the Non-pulsatile model

Consider the state equation given by

$$\begin{pmatrix} \dot{P}_a(t) \\ \dot{P}_v(t) \end{pmatrix} = \begin{pmatrix} -\frac{1}{c_a R} & \frac{1}{c_a R} \\ \frac{1}{c_v R} & -\frac{1}{c_v}(\frac{1}{r} + \frac{1}{R}) \end{pmatrix} \begin{pmatrix} P_a(t) \\ P_v(t) \end{pmatrix} + \frac{1}{c_a} HV_{\text{str}} \begin{pmatrix} 1 \\ 0 \end{pmatrix} \tag{14}$$

The determinant is $\frac{1}{c_a R}\frac{1}{c_v r} \neq 0$ and it easily follows that $HV_{\text{str}} r \begin{pmatrix} 1 + \frac{R}{r} \\ 1 \end{pmatrix}$ is a uniquely determine stationary point. Since it is uniquely determine by the heart rate, the stroke volume and the two resistances to flow, the stationary point may be used to estimate r and R independently of c_a and c_v. The characteristic polynomial becomes

$$\mathcal{P}(\lambda) = \lambda^2 - \left(\frac{1}{c_v r} + \frac{1}{R}(\frac{1}{c_a} + \frac{1}{c_v})\right)\lambda + \frac{1}{c_a R}\frac{1}{c_v r}$$

and the characteristic roots are both real and negative

$$\lambda_{\pm} = -\frac{1}{2}\left(\frac{1}{R}(\frac{1}{c_a} + \frac{1}{c_v}) + \frac{1}{c_v r}\right) \pm \sqrt{\frac{1}{4}\left(\frac{1}{R}(\frac{1}{c_a} + \frac{1}{c_v}) + \frac{1}{c_v r}\right)^2 - \frac{1}{c_a R}\frac{1}{c_v r}} \tag{15}$$

Notice that the system is asymptotically stable. The transient, which is determined by the characteristic roots, depends on the resistances, as well as the capacities. With the nominal values for the parameters, given in appendix, $\lambda_+ = -0.0283$ and $\lambda_- = -0.615$ seconds^{-1}, and the corresponding eigenvectors are $(-0.72, -0.69)$ and $(-1.00, 0.003)$, respectively. Then the characteristic times of the system becomes 35.4 and 1.63 seconds. So the

arterial part shows a fast transient whereas the venous part shows a relative slow transient.

Moreover, when H is considered as a control variable, the system given in equation (15) is completely linear controllable, since the controllability matrix has full rank (see for example Russel (1979) or Lee & Markus (1967))

$$\operatorname{rank}\begin{pmatrix} 1 & -\frac{1}{c_a R} \\ 0 & \frac{1}{c_v R} \end{pmatrix} = 2$$

This mens that there exist a control $H = H(t)$, defined over a finite interval $[t_0, t_1]$, which transfers the dynamical system from any initial state to any desired final state in the defined time interval. Hence, we can steer the state in any desirable way by choosing $H(t)$ suitable. Notice that one could as well have chosen V_{str} or HV_{str} as control variable.

When dealing with the question of observability one have to specify the observable quantity. In our case it seems naturally to choose the arterial blood pressure as observable, i.e. the observable y is given by

$$y = \begin{pmatrix} 1 & 0 \end{pmatrix} \begin{pmatrix} P_a(t) \\ P_v(t) \end{pmatrix} = P_a(t) \tag{16}$$

Then the system in equation (15) with observable given in equation (17) is completely linear observable, since the observability matrix has rank 2

$$\operatorname{rank}\begin{pmatrix} 1 & 0 \\ -\frac{1}{c_a R} & \frac{1}{c_a R} \end{pmatrix} = 2$$

This means that every initial state can be determined from the knowledge of the observable $y = P_a(t)$ over the considered time interval. Hence, measuring the arterial blood pressure completely determine the state. However investigations (see section 7) show that the physiological control mechanism is non-linear. Therefore linear control theory does not suffice and non-linear control theory is needed. Alternatively one may turn the system into a close-loop control system, by modeling the non-linear feedback mechanisms $H = H(P_a)$ and $V_{\text{str}} = V_{\text{str}}(P_a)$ directly.

6 Control Mechanisms of the Cardiovascular System

In this section we briefly discuss the control mechanisms of the cardiovascular system and, in particular, the baroreflex-feedback mechanism.

Blood pressure is controlled by a large number of control mechanisms. The entire control system is very complex and the individual parts normally interact in a complicate manner, Guyton (1981). However, the system may be divided into at least two categories, autoregulation, which is due to the hemodynamic properties of the cardiovascular system, and nervous control. The baroreflex-feedback mechanism, which we consider here, belongs to the latter category, and is a short-term blood pressure control mechanism.

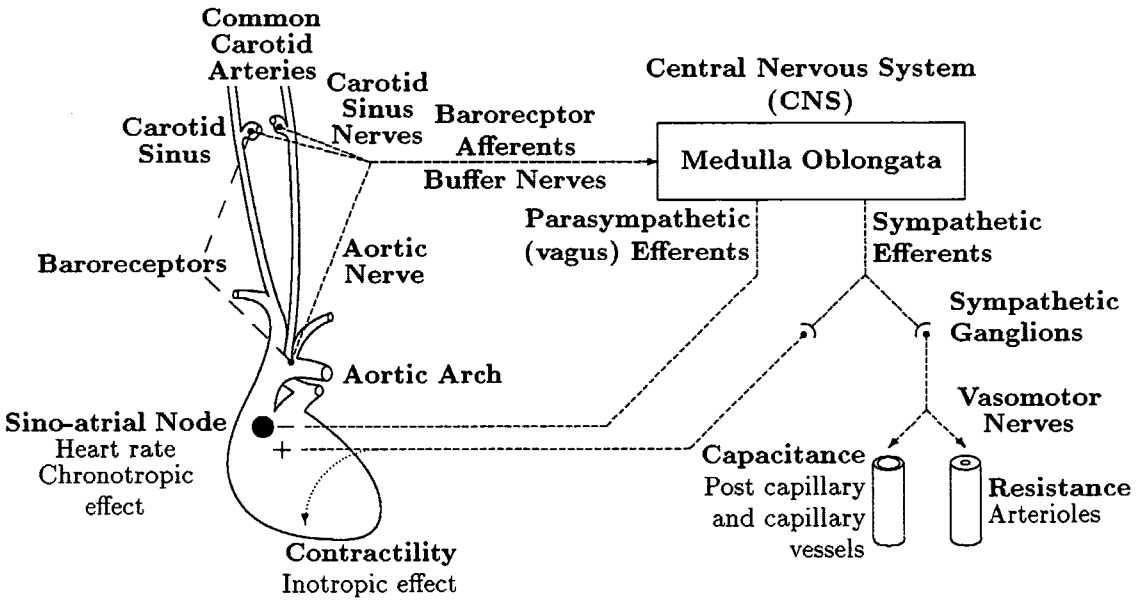

Figure 2: The baroreceptor feedback system.

The baroreceptors are tension-sensitive nerve fiber endings located at various places in the circulatory system. It is believed that those located in the aortic arch and in the carotid sinus are the most important ones, see figure 2. The baroreceptors sense the local pressure and cause a frequency in nerve activity. This nerve activity is transmitted, through the afferent nerve fibers, to the vegal center and the vasomotor center at medula oblongata in the central nervous system. The heart rate, the contractility and then the stroke volume of the ventricles, the peripheral resistances, and the arterial and venous capacities and unstressed volumes are controlled from the central nervous system, through the sympathetic and the parasympathetic nerve activity (see figure 2). All these control mechanisms serve to control the arterial pressure, i.e. to steer the pressure toward some "normal" set–point. Here, and throughout this paper, the term set-point denote a steady-state, determinated by physiological parameters of the model, toward which the pressure converge.

In the following we will only consider the system consisting of the arterial pressure, the baroreceptors, the nerve fibers going to the central nervous system, the central nervous system, the sympathetic and the parasympathetic nerve fibers going to the heart, the change in heart rate caused by the activity in these nerves (through the hormonal transmitters, norepinephine and acetylcholine) and in stroke volume (through contractility) caused by the activity in the sympathetic nerves. Moreover, we reserve the phrase "the baroreflex-feedback mechanism" to mean exactly this subsystem. In figure 3 we have sketched the cardiovascular system, as modeled earlier, together with this baroreflex-feedback mechanism.

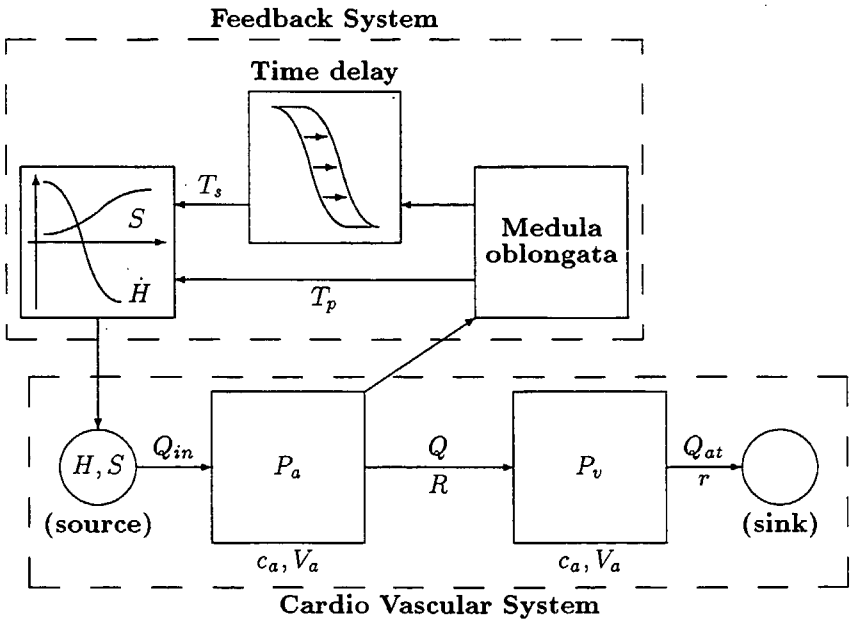

Figure 3: The controlled cardiovascular system.

To model the chronotropic effect of the baroreflex-feedback mechanism explicitly, we divide this system into two parts. The first part is described by the firing rate (nerve activity) of the nerve fibers, called the tones, at the nerve fiber endings going to the heart. The tones are functions of the arterial blood pressure. The second part is described by the change in heart rate as a function of the sympathetic and the parasympathetic tones. Measurements shows that there is a time-delay of the order of 10 seconds for the peak response (maximal effect) to appear in the sympathetic nervous system and of the order of less than 1 second in the parasympathetic nervous system, see Guyton & Harris (1951), Warner (1958), Warner & Russel (1969),

Korner (1971) Milhorn (1966) and Borst & Karemaker (1983). Hence the actual time-delay, assuming a simple one, is, in accordance with the measurements, a factor 10 times larger in the sympathetic system than in the parasympathetic system. This is because of the quick hydrolysis of the acetylcholine released by parasympathetic stimulation as compared with the slow reuptake and washout of the sympathetically released norepinephine in the heart. Therefore, we include the time-delay in the sympathetic nervous system and ignore that of the parasympathetic nervous system.In the litterature Warner (1958) and Warner & Russel (1969) estimate the time-delay to be in the range $[2,4]$ seconds, Cavalcanti et al. (1995) use $\tau = 2.5$ seconds, Rideout (1991) has $\tau \approx 3$ seconds (in Rideout it is an average value of a continuous delay), and Guyton & Harris (1951) estimate it to 13 seconds. Each of the above two parts is fairly well-known qualitatively, but quantitatively they are only roughtly known.

Less is known about how the inotropic effect of the baroreflex-feedback mechanism works. But it seems that the stroke volume increase slightly with the arterial mean pressure, through the sympathetic nerve system, in the physiological range under consideration.

7 Mathematical Model of the Baroreflex-Feedback Mechanism

In this section a mathematical model for the baroreflex-feedback mechanism, described in section 6, will be developed.

First we consider the chronotropic effect. As mentioned earlier we divide this feedback system into two parts.

The model describing the first part of this feedback mechanism is based on measurements of the sympathetic and the parasympathetic tones as functions of the arterial mean pressure, see Korner (1971) and references thererin. Graphs of the qualitative behavior of these functions are both sigmoidal in shape. It follows that the sympathetic tone T_s and the parasympathetic tone T_p is decreasing and increasing as functions of the arterial mean pressure, respectively, i.e.

$$T_s = g_s(P_a^\tau) \quad , g_s'(P_a^\tau) < 0,$$

$$T_p = g_p(P_a) \quad , \text{ and } g_p'(P_a) > 0$$

and

$$g_s \approx 1 \text{ for } P_a^\tau \text{ small}, \quad g_s \approx 0 \text{ for } P_a^\tau \text{ large},$$
$$g_p \approx 0 \text{ for } P_a \text{ small}, \quad \text{and } g_p \approx 1 \text{ for } P_a \text{ large}$$

where P_a^τ and P_a denotes the arterial mean pressure with and without time-delay, respectively, τ characterize the time-delay. Otherwise g_s and g_p are unspecified functions.

Example. As ad-hoc model one may choose

$$g_s(P_a^\tau) = \frac{1}{1 + (\frac{P_a^\tau}{\alpha_s})^{\beta_s}}$$

and

$$g_p(P_a) = \frac{1}{1 + (\frac{P_a}{\alpha_p})^{-\beta_p}}$$

where the parameters $\alpha_s, \alpha_p, \beta_s$ and β_p are all positive and characterize location and steepness of the curves, i.e.

$$g_s = \tfrac{1}{2} \text{ for } P_a^\tau = \alpha_s, \qquad g_p = \tfrac{1}{2} \text{ for } P_a = \alpha_p,$$

$$g_s' = -\tfrac{\beta_s}{4\alpha_s} \text{ for } P_a^\tau = \alpha_s, \quad \text{and } g_p' = \tfrac{\beta_p}{4\alpha_s} \text{ for } P_a = \alpha_p$$

Nominal values is $\alpha_s = \alpha_p = 93$ mmHg and $\beta_s = \beta_p = 7$ for a person at rest.

We emphasize that the phrase "mean pressure" in the pulsatile case may not mean the ordinary average value over a cycle, as in the non-pulsatile case, but rather a weighted average.

The model describing the second part of the chronotropic effect of the baroreflex-feedback mechanism is based on measurements of the change in heart rate as a function the tones, which may be found in a paper by Levy & Zieske (1969). From these measurements one may conclude that, the change in heart rate is an increasing function of the sympathetic tone and a decreasing function of the parasympathetic tone, and furthermore an increase in the parasympathetic tone will reduces the effect of the sympathetic tone on the change in heart rate. We write

$$\dot{H}(t) = h(T_s, T_p)$$

where

$$\frac{\partial h}{\partial T_s}(T_s, T_p) > 0 \text{ and } \frac{\partial h}{\partial T_p}(T_s, T_p) < 0$$

and

$$\frac{\partial h}{\partial T_s}(T_s, T_p) \text{ decrease wrt } T_p$$

Moreover, $h = \dot{H} < 0$ for $T_s \approx 0$ and $T_p \approx 1$, corresponding to high pressures, and $h = \dot{H} > 0$ for $T_s \approx 1$ and $T_p \approx 0$, corresponding to low pressures. Otherwise is h unspecified.

Example. As ad-hoc model one may choose

$$\dot{H}(t) = \frac{\alpha_H T_s}{1 + \gamma_H T_p} - \beta_H T_p$$

where the parameters α_H and β_H express the strength with which the sympathetic tone and the parasympathetic tone, respectively, influence the change in heart rate, and γ_H express the damping from the parasympathetic nervous system on the strength with which the sympathetic nervous system influence the change in heart rate. All parameters are positive. Notice that, $\dot{H} \approx -\beta_H < 0$ for high pressure and that $\dot{H} \approx \alpha_H > 0$ for low pressure. Nominal values is $\alpha_H = 0.84$ sec^{-2} and $\beta_H = 1.17$ sec^{-2}. This values reflect

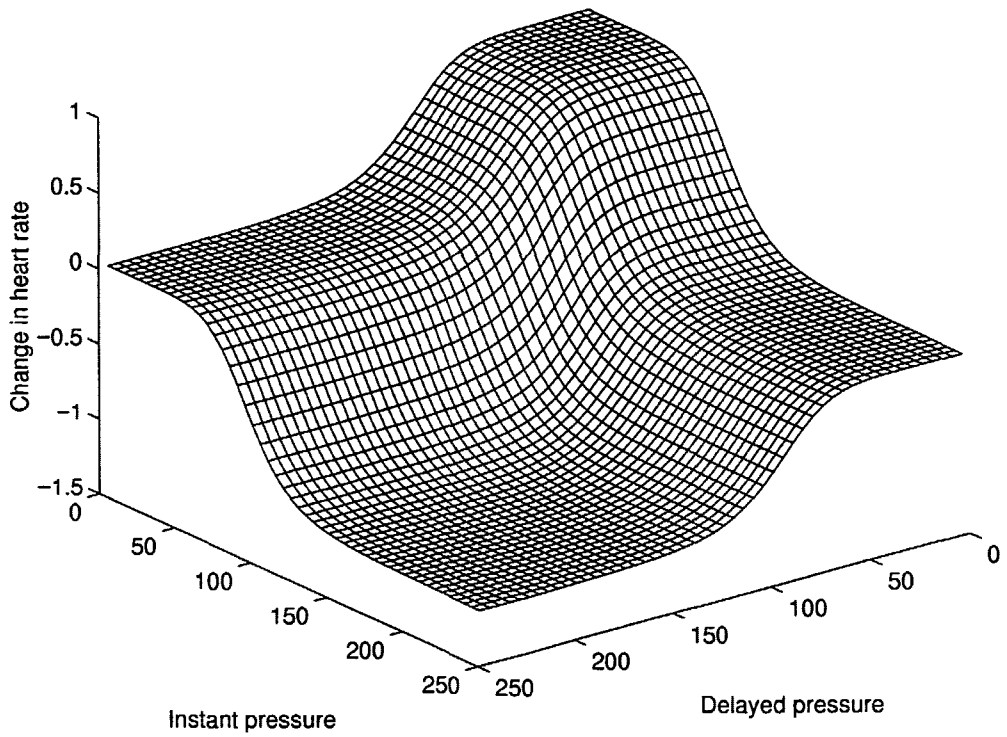

Figure 4: The Change in heart rate as a function of the delayed pressure P_a^τ and the instant pressure P_a.

the fact that at normal heart rate, the parasympathetic stimulation is more

dominant than the sympathetic stimulation, so the normal heart rate is lower than the intrinsic rate of the denervated heart. It turn out that h is little sensitive in γ_H, and one may choose $\gamma_H = 0$ to simplify the analysis.

Putting the above two submodels together in one model of the chronotropic effect of the baroreflex-feedback mechanism we obtain a non-linear differential equation with time-delay

$$\dot{H}(t) = f(P_a(t), P_a(t-\tau))$$

where it is used that the time-delay, in the non-pulsatile case, is given by $P_a^\tau(t) = P_a(t-\tau)$ and $f = h \circ g$. Hence, $\dot{H}$ is negative for high pressures and $\dot{H}$ is positive for low pressures. Furthermore, $\dot{H}$ is monotonic decreasing in each variable, i.e. $\frac{\partial f}{\partial P_a} < 0$ and $\frac{\partial f}{\partial P_a^\tau} < 0$. A typical behavior of the function f is shown in figure 4.

Combining the two ad-hoc submodels above it follows that the physiological parameters $\alpha_H, \beta_H, \alpha_s, \beta_s, \alpha_p$, and β_p determine the set-point for the steady state, see section 8. This function $f(P_a, P_a^\tau)$ for the nominal value of the parameters is shown in figure 4.

The inotropic effect of the baroreflex-feedback mechanism is less known than the chronotropic effect. From Suga et al. (1974) and Wesseling et al. (1982) it follows that the contractility S increase when P_a decrease, but at the same time t_s decrease. Following Allison et al. (1969), Suga et al. (1976) and Cavalcanti et al. (1995), V_{str} is approximately constant in the physiological range under consideration and is increasing with P_a for low pressure. However, we emphasize that this may variate very much, dependent of the athletic state of the considered person (for an athlete the contractility increase first and the heart rate secondly when exposed to exercise). It turn out that the following analysis do not change qualitatively whether V_{str} is constant or variate, as long as P_a is in the physiological range under consideration. But in case of variable V_{str} the analysis become more technical complicated. For simplicity we keep V_{str} fixed in what follows. Furthermore, it is not in general clear how the "set-point" for V_{str} behave qualitatively when the system is disturbed, but in some situations it is known. In agreement with this knowledge we assume that this "set-point" change similar to how the set-point for the heart rate change. In fact, we will only consider the case where the peripheral resistant increase exponentially, corresponding to a change from rest to exercise (a short term submaximal workload). In this case it is expected that the set-points behave similar. We return to this question in section 9.

We are now able to analyze the model of the close-loop control system of the cardiovascular system, which we will call the baroreflex-feedback model, given

by the model for the uncontrolled non-pulsatile cardiovascular system, described by equation (15), together with the model of the baroreflex-feedback mechanism just derived. This analysis will be carried out in the next section.

8 Analysis of the Baroreflex-Feedback Model

In this section we will analyse the baroreflex-feedback model given by the following system of non-linear differential equation with time-delay. Allowing variable stroke volume it follows from above

$$\begin{aligned} \dot{P}_a(t) &= -\tfrac{1}{c_a R} P_a(t) + \tfrac{1}{c_a R} P_v(t) + \tfrac{1}{c_a} V_{\text{str}}(P_a^\tau(t)) H(t) \\ \dot{P}_v(t) &= \tfrac{1}{c_v R} P_a(t) - (\tfrac{1}{c_v R} + \tfrac{1}{c_v r}) P_v(t) \\ \dot{H}(t) &= f(P_a(t), P_a(t-\tau)) \end{aligned} \tag{17}$$

Notice that the non-linearity and the time-delay do only appear through the feedback equations. Due to a well-known theorem (see for example El'sgol'ts & Norkin (1973)), continuity of f, g and ϕ, where ϕ is the initial condition in $[t_0 - \tau, t_0]$, guarantee existence of solution to equation (17). Moreover, if the right hand side of equation (17) is Lipschitz, uniqueness also follows. However, these general results are not needed here.

In the following we make the physiologically realistic assumptions on f, which are justified in section 7,

$$\begin{array}{l} f > 0 \text{ for } P_a \text{ and } P_a^\tau \text{ small,} \\ f < 0 \text{ for } P_a \text{ and } P_a^\tau \text{ large,} \\ f \text{ is differentiable, and} \\ \frac{\partial f}{\partial P_a} < 0 \text{ and } \frac{\partial f}{\partial P_a^\tau} < 0 \end{array} \tag{18}$$

We notice that when $P_a^\tau = P_a$ these assumption implies that

$$\begin{array}{l} f > 0 \text{ for } P_a \text{ small,} \\ f < 0 \text{ for } P_a \text{ large, and} \\ f \text{ is monotonic decreasing and continuous} \end{array} \tag{19}$$

In fact, it is the weaker assumptions (19) we are going to use, when we investigate the questions of existence and uniqueness of equilibria, in the following.

Theorem 1
Under the assumption (19) the system given by equation (17) has a uniquely determined equilibria.

Proof
We first notice that if the system is in an equilibria, then $P_a^\tau = P_a$. In this case we simply write $\dot{H} = f(P_a)$. By the assumptions, it follows that there exist a uniquely determined "set–point" value $P_a = P_\circ$, such that $f(P_\circ) = 0$. Then the system, given by equation (17), uniquely determinate P_v and H as

$$P_v(t) = \frac{1}{1 + \frac{R}{r}} P_\circ \tag{20}$$

and

$$H(t) = \frac{1}{RV_{\text{str}}(P_\circ)} \frac{1}{1 + \frac{r}{R}} P_\circ \tag{21}$$

where at equilibria $V_{\text{str}}(P_a(t)) = V_{\text{str}}(P_\circ) \equiv g(P_\circ)$. Hereby, the existence and uniqueness of an equilibria is shown. □

We emphasize that the proof for existence and uniqueness of an equilibria only use assumption (19) and the fact that the arterial pressure determine all the other state variables uniquely under equilibria.

Notice, that it follows from the proof that the ratio between the arterial mean pressure and the venous mean pressure is given by $1 + \frac{R}{r} \approx 16.4$ and that the ratio between the arterial mean pressure and the inflow is given by $R(1 + \frac{r}{R}) \approx 1.12$ mmHg sec/ml at the equilibria, i.e. in steady state.

Example. Continuing with the examples given in section 7 the so-called set-point becommes

$$P_\circ = \alpha_\circ (\frac{\alpha_H}{\beta_H})^{\frac{1}{\beta_\circ}}$$

for $\alpha_\circ = \alpha_s = \alpha_p$ and $\beta_\circ = \beta_s = \beta_p$ as in the case of the nominal values given in appendix. In the physiological estimated range $(\frac{\alpha_H}{\beta_H})^{\frac{1}{\beta_\circ}}$ is between 0.8 and 1.2 and $P_\circ \approx \alpha_\circ$.

We will now investigat the stability of the determinated equilibria and especially how this depends on the value of the time-delay and the feedback. But as mentioned the analysis is quite technical due to number of uncertain parameters when linearizing equation (17). However, it turns out that the qualitative behavior of the system agree with that where V_{str} is assumed constant. So for simplicity we will consider this case here and return to the full

feedback system in the discussion and when simulating data, obtained by an ergometer bicycle test, in section 9. Hence we consider the feedback system

$$\begin{aligned} \dot{P}_a(t) &= -\tfrac{1}{c_a R}P_a(t) + \tfrac{1}{c_a R}P_v(t) + \tfrac{1}{c_a}V_{\text{str}}H(t) \\ \dot{P}_v(t) &= \tfrac{1}{c_v R}P_a(t) - (\tfrac{1}{c_v R} + \tfrac{1}{c_v r})P_v(t) \\ \dot{H}(t) &= f(P_a(t), P_a(t-\tau)) \end{aligned} \tag{22}$$

with the unique equilibria $P_a = P_\circ$, $P_v(t) = \frac{1}{1+\frac{R}{r}}P_\circ$, and $H(t) = \frac{1}{RV_{\text{str}}}\frac{1}{1+\frac{r}{R}}P_\circ$.

Before examine the question of stability of the equilibria, it is appropriate to transform the system into dimensionless form. Consider the transformation $(P_a, P_v, H, t) \to (x_a, x_v, x_h, s)$, given by

$$\begin{aligned} P_a &= x_a P_0 \\ P_v &= x_v P_0 \\ H &= x_h \frac{c_a P_0}{V_{\text{str}} t_0} \\ t &= s t_0 \end{aligned}$$

where P_0 (≈ 100 mmHg) is the arterial equilibria pressure and $t_0 = c_a R$ (≈ 1.6 sec) is a characteristic time, whereby the number of parameters reduces. Then equation (17) transform into

$$\begin{aligned} \dot{x}_a &= -x_a + x_v + x_h \\ \dot{x}_v &= \alpha x_a - \beta x_v \\ \dot{x}_h &= \tilde{f}(x_a, x_a^\tau) \end{aligned} \tag{23}$$

where $\alpha = \frac{c_a}{c_v} \approx 3.0 \cdot 10^{-3}$, $\beta = \frac{c_a}{c_v}(1+\frac{R}{r}) \approx 16.4\alpha \approx 4.9 \cdot 10^{-2}$ and $\tilde{f}(x_a, x_a^\tau) = \frac{t_0^2 V_{\text{str}}}{P_0 c_a} f(x_a P_0, x_a^\tau P_0)$. Notice that $\tilde{f}$ and f share the same monotonic and sign properties. Hence, the equilibria of the system in equation (23) becomes

$$(x_a, x_v, x_h) = (1, \frac{1}{1+\frac{R}{r}}, \frac{1}{1+\frac{r}{R}})$$

Linearizing equation (23) in terms of the deviation from equilibria $(\overline{x}_a, \overline{x}_v, \overline{x}_h)$, under assumption (18), gives

$$\begin{aligned} \dot{\overline{x}}_a &= -\overline{x}_a + \overline{x}_v + \overline{x}_h \\ \dot{\overline{x}}_v &= \alpha \overline{x}_a - \beta \overline{x}_v \\ \dot{\overline{x}}_h &= -\gamma \overline{x}_a - \delta \overline{x}_a^\tau \end{aligned} \tag{24}$$

where $\gamma = -\frac{\partial \tilde{f}}{\partial x_a}(1,1)$ and $\delta = -\frac{\partial \tilde{f}}{\partial x_a^\tau}(1,1)$. Notice that all the appearing parameters are positive and that α only depend on the ratio of the compliances, and that β depend on this ratio as well as the ratio of the resistances. In case of the example above one get $\gamma \approx 2\beta_H$ and $\delta \approx 2\alpha_H$ assuming that $P_\circ = \alpha$ (the relative error made by this assumption is less than 10%).

We now write equation (24) as

$$\dot{x} + \mathbf{A}x + \mathbf{B}x^\tau = 0 \tag{25}$$

where x and x^τ denotes the transposed of $(\overline{x}_a, \overline{x}_v, \overline{x}_h)$ and $(\overline{x}_a^\tau, \overline{x}_v^\tau, \overline{x}_h^\tau)$, respectively, and

$$\mathbf{A} = \begin{pmatrix} 1 & -1 & -1 \\ -\alpha & \beta & 0 \\ \gamma & 0 & 0 \end{pmatrix} \quad \text{and} \quad \mathbf{B} = \begin{pmatrix} 0 & 0 & 0 \\ 0 & 0 & 0 \\ \delta & 0 & 0 \end{pmatrix}$$

The associated characteristic equation is then given by

$$\Delta(\lambda, \tau) = \det(\lambda \mathbf{I} + \mathbf{A} + \mathbf{B}e^{-\lambda\tau}) = P(\lambda) + Q(\lambda)e^{-\lambda\tau} = 0 \tag{26}$$

where

$$P(\lambda) = \lambda^3 + (\beta+1)\lambda^2 + (\gamma + \beta - \alpha)\lambda + \gamma\beta$$

and

$$Q(\lambda) = (\lambda + \beta)\delta$$

Notice that all coefficients in P and Q are positive, since $\beta > \alpha$, that P and Q are polynomials of degree 3 and 1, respectively, and that the only root, $\lambda_Q = -\beta$, in Q is negative and is not a root in P, since $P(\lambda_Q) = 2\beta(\beta - \frac{\alpha}{2} + \gamma) > 2\beta(\gamma - \alpha + \delta) > 0$. Moreover, $P(0) + Q(0) = \beta(\gamma + \delta) \neq 0$. Hence one may use the method outlined in the elegant paper of Cooke & van den Driessche (1986) to investigate stability of the equilibria. Notice first that the equilibria is stable for vanishing time-delay, i.e. $\tau = 0$, by the Rough-Hurwitz criteria. The characteristic polynomial is

$$\lambda^3 + (\beta+1)\lambda^2 + (\gamma + \delta + \beta - \alpha)\lambda + (\gamma + \delta)\beta$$

where all coefficients are positive and $(\beta+1)(\gamma+\delta+\beta-\alpha) - (\gamma+\delta)\beta = \gamma + \delta + (\beta+1)(\beta-\alpha)$ is positive. Secondly we seek positive roots y to

$$F(y) \equiv |P(iy)|^2 - |Q(iy)|^2$$

and afterward we solve equation (26) with respect to τ for these values of y, if any. Hereby we get a, possible infinite, sequence $\tau_n, n = 1, 2, \ldots$, at which

there may appear stability switches (Hopf bifucations). Calculating $F(y)$ one get

$$F(y) = y^6 + Ay^4 + By^2 + C$$

where

$$\begin{aligned} A &= (\beta+1)^2 - 2(\gamma+\beta-\alpha) \\ B &= (\gamma+\beta-\alpha)^2 - 2\gamma\beta(\beta+1) - \delta^2 \\ C &= (\gamma^2-\delta^2)\beta^2 \end{aligned}$$

Notice that this is a polynomial of third degree $\tilde{F}(z)$ in $z = y^2$. So we are looking for positive roots of $\tilde{F}(z)$, corresponding to positive roots $y = \sqrt{z}$ of $F(y)$, and especially is the number of such of interest. The roots of $\tilde{F}(z)$ depends continuously on the four parameters $(\alpha, \beta, \gamma, \delta)$. We divide the parameter space $\mathbf{R}^4_+$ into regions by hypersurfaces, such that the points of each region correspond to polynomials $\tilde{F}(z)$ with the same number of positive roots. In general there is four regions, which we denote O, I, II and III corresponding to none, one, two and three positive roots, respectively. Since α and β are fairly well estimated, $\alpha = 3.0 \cdot 10^{-3}$ and $\beta = 4.9 \cdot 10^{-2}$, we will consider these as known in the following typical scenario. Then the discussion reduces to the 2-dimensional (γ, δ)-parameter space $\mathbf{R}^2_+$, where the regions are separated by curves. The parameter space is divided naturally into two subspaces, $C < 0$ and $C > 0$, corresponding to $\delta > \gamma$ and $\delta < \gamma$, respectively. By Descartes' theorem, Descartes (1954(originally 1637)), it follows that the regions of one and three positive roots are located in the subspace $\delta > \gamma$, and those of none and two positive roots are located in the subspace $\delta < \gamma$. Moreover, by Descartes' theorem, three positive roots demand that $A < 0$, $B > 0$ and $C < 0$. These demands are inconsistent with the expressions for A, B and C. Therefore, there is one positive root if and only if $\delta > \gamma$. The boundary between regions O and II is characterized by that there is one non-positive root and one positive double root. Simulations show that these curves and regions are low sensitive to the exact values of α and β. However, below it is shown that the specific value of the solutions to equation (26) are indeed sensitive to the exact values of α and β. Figure 5 shows the numerical computed regions for the estimated values of α and β.

A first rough estimate for γ and δ is $\gamma = 2.34$ and $\delta = 1.67$. However, these estimates are with some uncertainty, and we may only expect that $\gamma \in [1, 6]$ and $\delta \in [1, 6]$. Hence, none of the possibilities none, one, and two positive roots can, at present, be excluded. Therefore we briefly sketch what happen in each of these regions:

O) If there are no positive roots of $\tilde{F}(z)$, the equilibria stay stable for all values of $\tau \geq 0$, since it is stable for $\tau = 0$, and no stability switches can

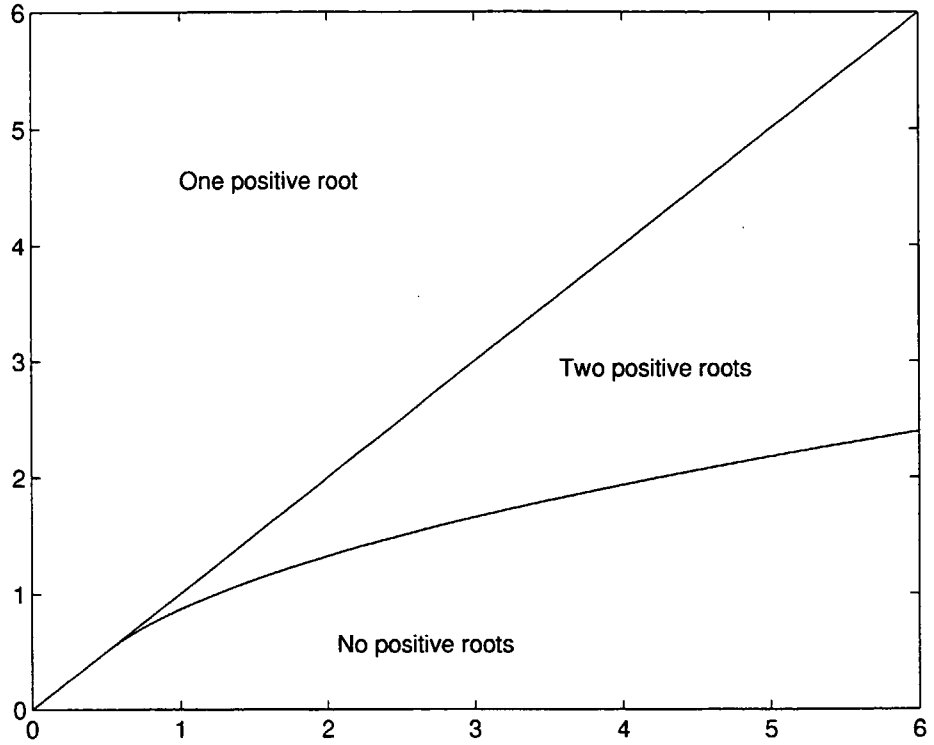

Figure 5: The regions of different numbers of positive roots in the (γ, δ)-parameter space.

occur. However, the physiologically realistic range has no intersection with region O.

Example o) $\gamma = 2.3$ and $\delta = 1.4$ In this case there are no positive roots, in fact there is only one real root of $\tilde{F}(z)$, $z = -0.024$. So in this case the equilibria is stable for all values of $\tau \geq 0$.

I) If there is precisely one positive simple root, say z_1, of $\tilde{F}(z)$, then there exist an infinite sequence, $\{\tau_n\}_{n=0}^{\infty}$, $\tau_n = \tau_0 + n\frac{2\pi}{y_1}$, $n \in \mathbf{N}$, with $y_1 = \sqrt{z_1}$, such that the pairs (y_1, τ_n) solves equation (26). When τ, considered as a parameter, runs from zero to infinity, there may appear stability switches for $\tau = \tau_n$. Since the equilibria is stable for $\tau = 0$ it follows that it loose its stability at $\tau = \tau_0$ and stay unstable for $\tau > \tau_0$. Then there is only one stability window, $[0, \tau_0[$, in this case. Numerical considerations shows that in the case of one positive simple root, $\tau_0 < 0.5$ second, for $\gamma, \delta \in [1, 6]$, as in example *i)* below. Therefore, this case seems to be excluded as physiologically realistic, since τ experimentally is estimated to be in the range $[1, 4]$ seconds.

Example i) $\gamma = 4.36$ and $\delta = 4.84$. In this case there is one positive root, $z_1 = 8.24$, of $\tilde{F}(z)$, corresponding to $y_1 = 2.87$. Then equation (26) gives $\tau_0 = 0.35$ seconds. So in this case the equilibria is stable only for $\tau \in [0, 0.35[$ and unstable else. The frequency for $\tau = 0.35$ seconds is 0.3 Hz.

II) If there are precisely two positive simple roots of $\tilde{F}(z)$, say z_1 and z_2, with $z_1 > z_2$, there exist two infinite sequences $\{\tau_n^1\}_{n=0}^{\infty}$ and $\{\tau_n^2\}_{n=0}^{\infty}$, $\tau_n^1 = \tau_0^1 + n\frac{2\pi}{y_1}$ and $\tau_n^2 = \tau_0^2 + n\frac{2\pi}{y_2}$, $n \in \mathbf{N}$, with $y_1 = \sqrt{z_1}$ and $y_2 sqrt z_2$, such that the pairs (y_1, τ_n^1) and (y_2, τ_n^2) solves equation (26). Since $y_1 > y_2$ the equilibria becomes unstable at $\tau = \tau_0^1$, stable again at $\tau = \tau_0^2$ (if $\tau_0^1 < \tau_0^2$), and so on, alternating between stable and unstable, until $\tau = \tau^* = \tau_n^1$ for some finite n. This is a consequence of the fact that $\frac{2\pi}{y_1} < \frac{2\pi}{y_2}$, so destabilization switches occur, on average, more frequently than stabilization switches. In fact, there appear

$$n^* = \left[\frac{\tau_0^1 - \tau_0^2 + \frac{2\pi}{y_2}}{2\pi(\frac{1}{y_2} - \frac{1}{y_1})} \right]$$

stability windows and n^* windows of instability (here the square brackets denote the smallest integer larger than the number in the brackets). The length of the first stability window $[0, \tau_0^1[$ is τ_0^1, the length of the $(n+1)$'th stability window is

$$\tau_0^1 - \tau_0^2 + \frac{2\pi}{y_1} + n \cdot 2\pi(\frac{1}{y_1} - \frac{1}{y_2})$$

for $n = 1, 2, \ldots, n^* - 1$, and the length of the n'th window of instability is

$$\tau_0^2 - \tau_0^1 + (n-1) \cdot 2\pi(\frac{1}{y_2} - \frac{1}{y_1})$$

for $n = 1, 2, \ldots, n^* - 1$ The last window of instability is $[\tau^*, \infty[$, where $\tau^* = \tau_{n^*}^1$. As shown in the examples below two stability windows are likely (within the physiologically parameter range $\gamma, \delta \in [1, 6]$), one with possible values of τ less than 0.5 seconds, and the other with window included in $[3, 7]$ seconds.

Example ii) $\gamma = 5.22$ and $\delta = 4.80$. In this case there are two positive roots, $z_1 = 4.4$ and $z_2 = 84$, of $\tilde{F}(z)$, corresponding to $y_1 = 2.1$ and $y_2 = 9.2$, respectively. Then equation (26) gives $\tau_0^1 = 0.36$ and $\tau_0^2 = 7.02$ seconds. Therefore there appear two destability switches, at $\tau_0^1 = 0.36$ and at $\tau_1^1 = 3.71$ seconds, before any stability switches (the first one at $\tau_0^2 = 7.02$), So in this case there is only one stability window, $[0, 0.36[$. As in example *i)* we conclude that this case seems to be physiologically unrealistic.

Example ii') $\gamma = 5.56$ and $\delta = 4.24$. In this case there are two positive roots, $z_1 = 8.4$ and $z_2 = 1.44$, of $\tilde{F}(z)$, corresponding to $y_1 = 2.9$ and

$y_2 = 1.2$, respectively. Then equation (26) gives $\tau_0^1 = 0.42$ and $\tau_0^2 = 3.7$ seconds. So in this case there is two stability windows $[0, 0.42[$ and $[3.7, 3.8[$ seconds, and two windows of instability $[0.42, 3.7[$ and $[3.8, \infty[$ (qualitatively the system is equivalent to that shown in figure 6). The frequency is 2 Hz for $\tau = 0.42$ seconds and 5 Hz for $\tau = 3.7$ seconds. We conclude that this case is physiologically unrealistic due to the large frequency.

Example ii") $\gamma = 2.34$ and $\delta = 1.67$. In this case there are two positive roots, $z_1 = 2.67$ and $z_2 = 1.00$, of $\tilde{F}(z)$, corresponding to $y_1 = 1.64$ and $y_2 = 1.00$, respectively. Then equation (26) gives $\tau_0^1 = 1.34$ and $\tau_0^2 = 4.00$ seconds. So in this case there is two stability windows $[0, 1.34[$ and $[4.00, 7.49[$ seconds, and two windows of instability $[1.34, 4.00[$ and $[7.49, \infty[$, see figure 6. The oscillation frequency for $\tau = 4.00$ seconds is 0.1 Hz. We conclude that this case seems to be physiologically realistic.

From these stability considerations we conclude that $\gamma \geq \delta$, since otherwise we are in case *I)*, which gives physiologically unrealistic results for $\gamma, \delta \in [1, 6]$.

At this point we emphasize that the solutions of the characteristic equation (26) depends on the parameters, i.e. the compliances and the resistances. It turn out that the system may be unstable (oscillatory) for some values of the time-delay τ and then become stable for the same time-delay by, for example, a decrease in the peripheral resistance, see figure 7. The reason for this is the exact location of the stability and instability windows are sensitive to the parameters. The windows moves continuously with the values of the parameters.

It is known, Wesseling et al. (1982), Koepchen (1984) and Cavalcanti et al. (1995), that the arterial mean pressure is in fact not in a steady state but rather is oscillatory, approximately with a frequency of 0.1 Hz and an amplitude less than 10 mmHg. In the literature these oscillations are known as the 10 seconds Mayer waves, Seidel & Herzel (1995). In the litterature it is suggested that such 10 seconds Mayer waves may be caused by the time-delay. If we demand the bifucation frequency, the frequency at the stability switches, to be 0.1 Hz (Mayer waves), then equation (26) gives

$$\delta = \frac{1}{\sin(\tau)}$$

and

$$\gamma = 1.0 - \cot(\tau)$$

From this it follows that the physiological range of τ, demanding a bifucation frequency of 0.1 Hz, is $]\frac{\pi}{4}, \pi[\approx]1.26, 5.03[$ seconds. For $\tau = 4$ seconds one get

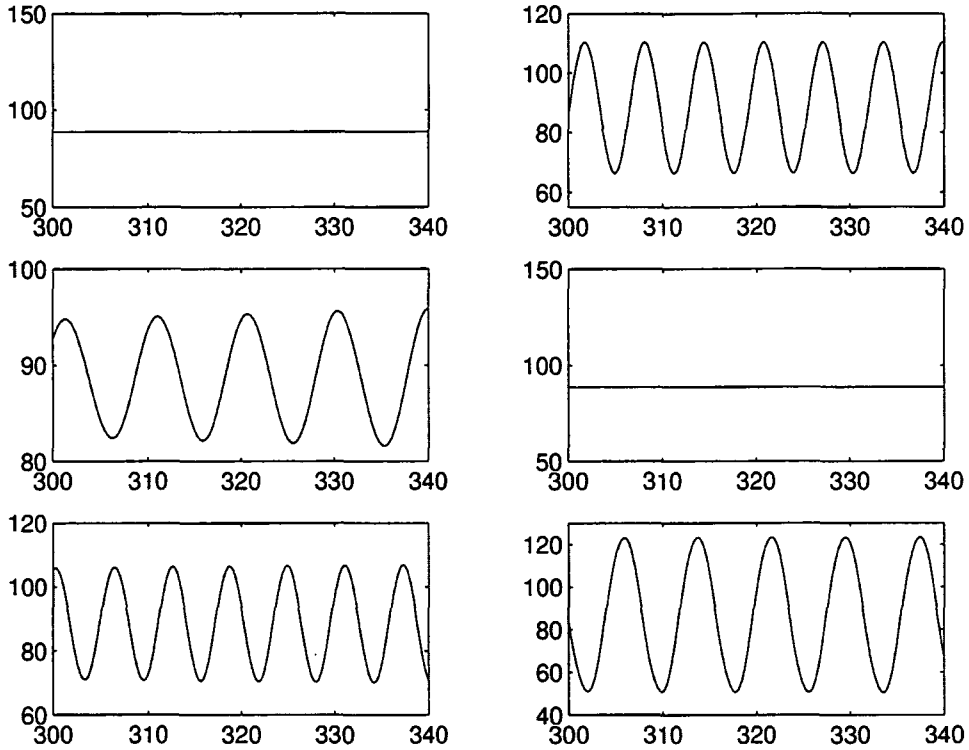

Figure 6: The arterial pressure $P_a(t)$ in mmHg vs. time in seconds for six different values of the time-delay. Upper left: $\tau = 1.0$ seconds, upper right: $\tau = 1.4$ seconds, middle left: $\tau = 3.9$ seconds, middle right: $\tau = 5.0$ seconds, lower left: $\tau = 7.5$ seconds, lower right: $\tau = 10.0$ seconds. For $\tau = 3.9$ seconds one observe oscilations with a frequency of 0.1 Hz and an amplitude of 7 mmHg, as in the case of Mayer waves. The values of the parameters are $\alpha_H = 0.84$ seconds^{-2}, $\beta_H = 1.17$ seconds^{-2}, $\alpha_s = \alpha_p = 93$ mmHg and $\beta_s = \beta_p = 7$.

$\delta = 1.67$ and $\gamma = 2.34$ or correspondingly $\alpha_H \approx 0.84$ sec^{-2} and $\beta_H \approx 1.17$ sec^{-2}, as were chosen as our first rought estimates. The system is oscillatory corresponding to the value of τ belongs to an instability window, see figure 6. However our simulations shows that the oscillations are sensitive to change in the parameters, for example the peripheral resistance. In fact, if we decrease the peripheral resistance by 20% then the oscillations may disappear, corresponding to the window of instability, which τ belongs to, moves away such that τ then belongs to a window of stability, this is shown in figure 7. Hence we suggest an experiment which shows the sensitivity of the 10 seconds Mayer waves on the parameters, especially on the peripheral resistance. Such an experiment could determinate whether or not the 10

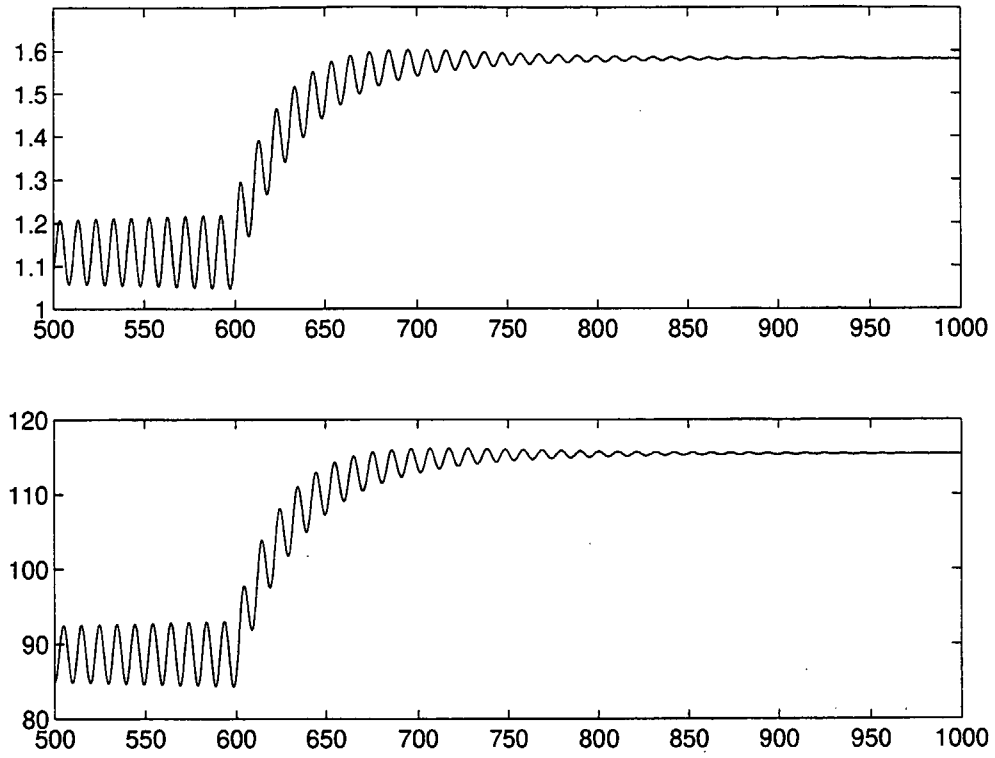

Figure 7: Oscillations in the heart rate $H(t)$ in seconds^{-1} (upper) and in arterial pressure $P_a(t)$ in mmHg (lower), vs. time in seconds, are sensitive to the value of the peripheral resistance. At time $t = 600$ seconds the peripheral resitance decrease exponentially by 20%. Before $t = 600$ seconds one observe oscilations with a frequency of 0.1 Hz and an amplitude of 5 mmHg, as in the case of Mayer waves. After $t = 600$ the oscillations vanish. The values of the parameters are $\alpha_H = 0.84$ seconds^{-2}, $\beta_H = 1.17$ seconds^{-2}, $\alpha_s = \alpha_p = 93$ mmHg and $\beta_s = \beta_p = 7$ and the time-delay is $\tau = 4.0$ seconds.

second Mayer waves is due to time-delay.

When considering the full feedback system, including the stroke volume as a non-constant function, the coefficients A, B and C in the six order polynomial $F(y)$ becomes

$$\begin{aligned} A &= (\beta+1)^2 - 2(\eta\gamma + \beta - \alpha) - \xi^2 \\ B &= (\eta\gamma + \beta - \alpha)^2 - 2\eta\gamma\beta(\beta+1) - \beta^2\xi^2 - \eta^2\delta^2 \\ C &= (\gamma^2 - \delta^2)\eta^2\beta^2 \end{aligned}$$

where η and ξ are two parameters characterizing the inotropic effect. Numerical analysis shows that there appear regions in typical planes parallel to

two axis in the 4-dimensional $(\gamma, \delta, \eta, \xi)$-parameter space $\mathbf{R}^4_+$ similar to those described for the (γ, δ)-parameter space above (figure 5).

We finally end this section by notice that the approximation $r = 0$ in equation (5) reduces the equations (13)-(14), describing the uncontrolled non-pulsatile systemic part of the cardiovascular system, to the well-known equation from the classical Windkessel model

$$\dot{P}_a(t) = -\frac{1}{c_a R} P_a + \frac{V_{\text{str}}}{c_a} H$$

Together with the feedback mechanism described in section 7 one get an analytically more manageble system. Then theorem 1 and the proof takes over, with equilibria given by $P_a = P_o$, for some set-point value P_o, and $H = H_o = \frac{1}{RV_{\text{str}}} P_o$ (which is equation (22) in the limit $r \to 0$). Then direct calculations gives that the (γ, δ)-parameter space are divided into region quite similar to what is shown in figure 5. The curves dividing the regions then become $\gamma = \delta$ and the part of the parabola $\gamma = \delta^2 + \frac{1}{4}$ where $\gamma > \frac{1}{2}$. However, the resulting stability windows and the discussion thereof become similar to what we got without the approximation $r = 0$.

In next section we turn to simulations and verification by use of experimental data.

9 Simulation and Verification

In this section we show how the model respond to a decrease in peripheral resistance. In Kappel & Peer (1993) simulations, obtained by use of their model, was compared to data obtained in a bicycle ergometer test. Such a short term submaximal workload is assumed to affect the peripheral resistance only. Simulations shows that the peripheral resistance respond to a sudden step increase in workload by decreasing exponentially with a time-constant of approximately 30 seconds. Figure 8 shows the respond of the model, presented in this paper, to such a 20% decrease in peripheral resistance. The simulation obtained by use of our model agree, to a satisfactory degree, with the experimental data given, despite the choice of a very simple model for the uncontrolled cardiovascular system. Furthermore the venous pressure and the stroke volume behave as expected. Taken into account the large individual variation, for example due to the athletic state of the person used in the experiment, we conclude that the model provides a satisfactory decription.

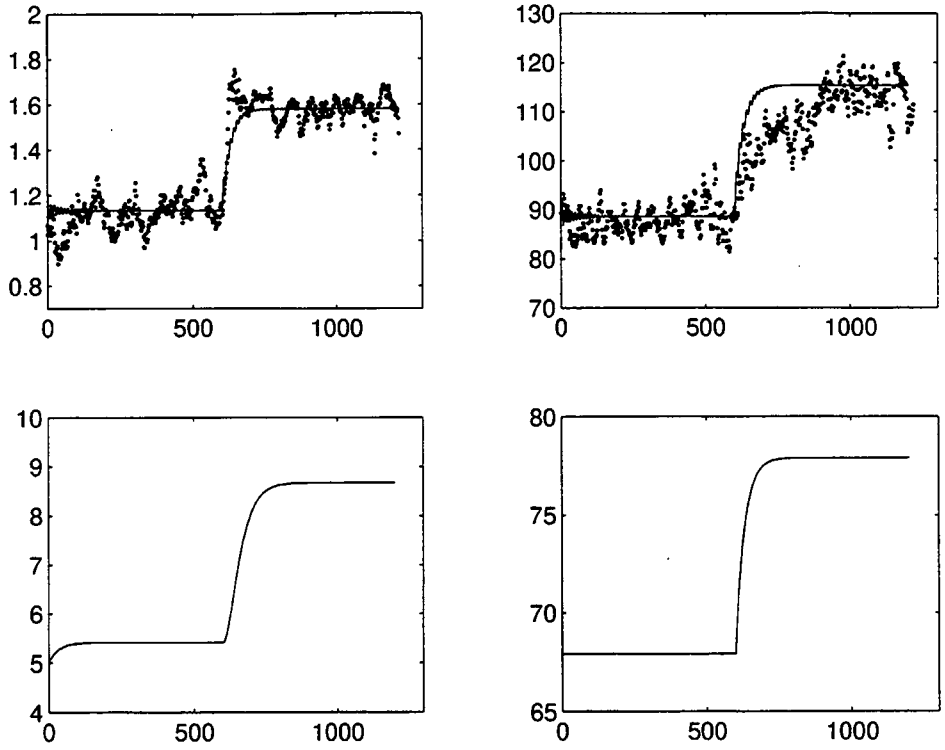

Figure 8: How the model of the cardiovascular system respond to an exponential decrease in peripheral resistance, by 20% from 1.05 mmHg sec/ml to 0.84 mmHg sec/ml. In this simulation we have used $\tau = 5.0$ seconds only to avoid oscilations in steady state. Solid curves represent simulations and dots represent data, obtained by Kappel & Peer (1993) (with permission). Upper left shows heart rate $H(t)$ in seconds^{-1} vs. time t in seconds, upper right shows arterial pressure $P_a(t)$ in mmHg vs. time t in seconds, lower left shows the venous pressure P_v in mmHg vs. time t in seconds, and lower right shows the stroke volume $V_{\text{str}}(t)$ in ml vs. time t in seconds. The parameter values are $\alpha_H = 0.84$ seconds^{-2}, $\beta_H = 1.17$ seconds^{-2}, $\alpha_s = \alpha_p = 93$ mmHg and $\beta_s = \beta_p = 7$.

10 Discussion, Summary and Outlook

We present a direct modelling of the chronotropic and inotropic parts of the non-linear baroreflex-feedback mechanism. The modelling include a description of both the sympathetic and parasympathetic nerve system, including time-delay. This modelling is based on physiological theory and empirical facts, to our knowledge for the first time.

The model of the feedback mechanism is evaluated on an expanded, but simple, Windkessel model of the cardiovascular system. Stability, with special attention to the effect of the value of the time-delay, is analyzed. The analysis show that it is likely that there appear several windows of stability separated by windows of instability wrt. the time-delay τ. Moreover, the exact location of these windows are sensitive to the value of the other parameters in the model. It is shown that a 20% decrease in peripheral resistance, as is likely when a person is going from rest to exercise (with a workload of approximately 50 Watt), might change the pattern and location of these stability and instability windows. Then the state of the system may change from being instable, i.e. oscilatory, to be stable, or vice versa. At the stability switches a Hopf bifucation takes place. Near to the stability switches in one direction the system is in or approach a stable steady state and in the opposite direction the state perform oscilations. For physiological realistic time-delays, for example $\tau = 4$ seconds, the system perform oscilations with a frequency of 0.1 Hz and an amplitude less than 10 mmHg, as in the case of Mayer waves. However, these oscilations are sensitive to variations in the parameters, as described above. Hereby a simple clinical experiment is suggested to decide whether or not the Mayer waves originate from time-delay. Finally we simulate data obtained in a bicycle ergometer test. This shows a satisfactory agreement between data and simulation results concerning the heart rate and the mean arterial pressure. Also the simulation shows the expected behavior of the venous pressure and the stroke volume.

Based on our investigation we conclude that our model of the baroreflex-feedback mechanism catch on to the major effect of the real physiological mechanism being modelled. Hereby we get the possibility of improve our knowledge of real system being modelled.

In near future at least three aspects will be investigated. How does a limit in the work performed by the heart affect the analysis and the conclusions ? How do the ignored effects of the baroreflex-feedback mechanism, i.e. the effect on the peripheral resistance and on the venous pool, influence both the model and the results ? How will a pulsatile system behave when imposed our feedback model ? In fact a major point is that with our choice of approach these and other question is able not only to be stated but also answered.

Appendix

Below we bring two lists, one of the various nominal values of the parameter used in the uncontrolled model and the other of the various nominal values

of the parameters used in the feedback model. When a parameter differ in value between rest phase and exercise phase the first value denote the value at the rest phase and the second value typed in brackets denote the value at the exercise phase. The values for the peripheral resistance and the stroke volume approach their value at the exercise phase asymptotically. The data given in the list of parameters used in the uncontrolled model agree with those in the literature and with physiological estimated values.

Nominal values of parameters in the uncontrolled model:

Arterial conpliance $c_a = 1.55$ ml/mmHg
Venous compliance $c_v = 519$ ml/mmHg
Peripheral resistance $R = 1.05(0.84)$ mmHg sec/ml
Venous outflow resistance $r = 0.068$ mmHg sec/ml
Stroke volume $V_{\mathrm{str}} = 67.9(77.9)$ ml
Typical mean heart rate $H = 1.24$ sec^{-1}
Typical mean arterial pressure $P_o = 100$ mmHg
Typical mean venous pressure $P_{v,o} = 7$ mmHg

Nominal values of parameters in the feedback model:

$\alpha = \frac{c_a}{c_v} = 3.0 \cdot 10^{-3}$
$\beta = \frac{c_a}{c_v}(1 + \frac{R}{r}) = 4.9 \cdot 10^{-2}$
$\alpha_o = \alpha_s = \alpha_p = 93(121)$ mmHg
$\beta_o = \beta_s = \beta_p = 7$
$\alpha_H = 0.84$ sec^{-2}
$\beta_H = 1.17$ sec^{-2}
$\gamma_H = 0$

References

Allison, J., Sagawa, K. & Kumada, M. (1969). An open-loop analysis of the aortic arch barostatic reflex, *American Journal of Physiology* **217**.

Berger, S. (1993). Flow in large blood vessels, *Contemporary Mathematics* **141**.

Borst, C. & Karemaker, M. (1983). Time delays in the baroreceptor reflex, *Journal of the Autonomic Nervous System* **9**.

Cavalcanti, S., Belardinelli, E. & Severi, S. (1995). Numerical simulation of the short-term heart regulation, *in* H. Power & R. Hart (eds), *Computer Simulations in Biomedicine*, Computational Mechanics Publications.

Cooke, K. & van den Driessche, P. (1986). On zeroes of some transcendental equations, *Funkcialaj Ekvacioj* **29**.

El'sgol'ts, L. & Norkin, S. (1973). *Introduction to the Theory and Application of Differential Equations with Deviating Arguments*, Academic Press.

Grodins, F. (1959). Intergrative cardiovascular physiology: A mathematical synthesis of cardiac and blood vessel hemodynamics, *The Quarterly Review of Biology* **34**(2).

Grodins, F. (1963). *Control Theory and Biological systems*, Columbia University Press.

Guyton, A. (1981). *Textbook of Medical Physiology*, sixth edn, W.B. Saunders Company.

Guyton, A. & Harris, J. (1951). Pressoreceptor-autonomic oscillation: A probable cause of vasomoter waves, *American Journal of Physiology* **165**.

Kappel, F. & Peer, R. (1993). A mathematical model for fundamental regulation processes in the cardiovascular system, *Journal of Mathematical Biology* **31**.

Koepchen, H. (1984). History of studies and concepts of blood pressure waves, *in* K. Miyakawa, H. Koepchen & C. Polosa (eds), *Mechanisms of Blood Pressure*, Springer-Verlag.

Korner, P. (1971). Integrative neural cardiovascular control, *Physiological Review* **51**(2).

Lee, E. & Markus, L. (1967). *Foundation of Optimal Control Theory*, John Wiley and sons.

Levy, M. & Zieske, H. (1969). Autonomic control of cardiac pacemaker, *Journal of Applied Physiology* **27**.

Milhorn, H. (1966). *The Application of Control Theory to Physiological Systems*, W.B. Saunders Company.

Murdock, J. (1991). *Pertubations, Theory and Methods*, John Wiley & Sons, Inc.

Noldus, E. (1976). Optimal control aspects of left ventricular ejection dynamics, *Juornal of Theoretical Biology* **63**.

Noordergraaf, A. (1978). *Circulatory System Dynamics*, Academic Press.

Olufsen, M. & Ottesen, J. (1995). Outflow conditions in human arterial flow, *in* H. Power & R. Hart (eds), *Computer Simulations in Biomedicine*, Computational Mechanics Publications.

Ono, K., Uozumi, T., Yoshimoto, C. & Kenner, T. (1982). The optimal cardiovascular regulation of the arterial blood pressure, *Cardiovascular System Dynamics; Model and Measurements*, Plenum Press.

Pedley, T. (1980). *The Fluid Mechanics of Large Blood Vessels*, Cambridge University Press.

Peskin, C. (1976). *Partial Differential Equations in Biology*, Lecture Notes from CIMS (Courant Institute of Mathematical Sciences), New York.

Rideout, V. (1991). *Mathematical and Computer Modeling of Physiological Systems*, Medical Physics Publishing.

Russel, D. (1979). *Mathematics of Finite-Dimensional Control Systems - Theory and Design*, Marcel Dekker.

Seidel, H. & Herzel, H. (1995). Modelling heart rate variability due to respiration and baroreflex, *in* E. Mosekilde & O. Mouritsen (eds), *Modelling the Dynamics of Biological Systems, Nonlinear Phenomena and Pattern Formation*, Springer-Verlag.

Sir Lighthill, J. (1975). *Mathematical Biofluiddynamics*, Society for Industrial and Applied Mathematics.

Suga, H., Sagawa, H. & Kostiuk, D. (1976). Controls of ventricular contractility assessed by pressure-volume ratio, e_{max}, *Cardiovascular Research* **10**.

Suga, H., Sagawa, H. & Shoukas, A. (1974). Carotid sinus baroreflex effects on instantanious pressure-volume ratio of the canine left ventricle, *Journal of Physiologycal Society of Japan* **36**.

Taylor, M. (1978). Optimality priciples applied to the design and control mechanisms of the vascular system, *The Arterial System; Dynamics, Control Theory and Regulation*, Springer-Verlag.

Tham, R.-Y. (1988). *A Study of Effects of Halothane on Canine Cardiovascular System and Baroreceptor Control*, PhD thesis, University of Wisconsin-Madison. Xerographic printed by UMI Dissertation Services, A Bell & Howell Company, 1995.

Usino, M. (1995). A mathematical model of the interaction between arterial and cardiopulmonary baroreceptors during acute cardiovascular stress, *in* H. Power & R. Hart (eds), *Computer Simulations in Biomedicine*, Computational Mechanics Publications.

Warner, H. (1958). The frequency-denpendent nature of blood pressure regulation by carotid sinus studied with an electic analog., *Circulation Research* **VI**.

Warner, H. (1962). Use of analogue computers in the study of control mechanisms in the circulation., *Federation Proceedings* **21**.

Warner, H. & Cox, A. (1962). A mathematical model of heart reate control by sympthetic and vagus efferent information, *Jounal of Applied Physiology* **17**.

Warner, H. & Russel, R. (1969). Effect of combined sympathetic and vagal stimulation on heart rate in the dog, *Circulation Research* **XXIV**.

Wesseling, K. et al. (1982). Baronodulation as the cause of short term blood pressure variability, *in* G. Alberi, Z. Bajzer & P. Baxa (eds), *Applications of Physics to Medicine and Biology*, Wold Scientific.

Liste over tidligere udkomne tekster tilsendes gerne. Henvendelse herom kan ske til IMFUFA's sekretariat tlf. 46 75 77 11 lokal 2263

217/92 "Two papers on APPLICATIONS AND MODELLING IN THE MATHEMATICS CURRICULUM"
by: Mogens Niss

218/92 "A Three-Square Theorem"
by: Lars Kadison

219/92 "RUPNOK - stationær strømning i elastiske rør"
af: Anja Boisen, Karen Birkelund, Mette Olufsen
Vejleder: Jesper Larsen

220/92 "Automatisk diagnosticering i digitale kredsløb"
af: Bjørn Christensen, Ole Møller Nielsen
Vejleder: Stig Andur Pedersen

221/92 "A BUNDLE VALUED RADON TRANSFORM, WITH APPLICATIONS TO INVARIANT WAVE EQUATIONS"
by: Thomas P. Branson, Gestur Olafsson and Henrik Schlichtkrull

222/92 On the Representations of some Infinite Dimensional Groups and Algebras Related to Quantum Physics
by: Johnny T. Ottesen

223/92 *THE FUNCTIONAL DETERMINANT*
by: Thomas P. Branson

224/92 *UNIVERSAL AC CONDUCTIVITY OF NON-METALLIC SOLIDS AT LOW TEMPERATURES*
by: Jeppe C. Dyre

225/92 *"HATMODELLEN" Impedansspektroskopi i ultrarent en-krystallinsk silicium*
af: Anja Boisen, Anders Gorm Larsen, Jesper Varmer, Johannes K. Nielsen, Kit R. Hansen, Peter Bøggild og Thomas Hougaard
Vejleder: Petr Viscor

226/92 *"METHODS AND MODELS FOR ESTIMATING THE GLOBAL CIRCULATION OF SELECTED EMISSIONS FROM ENERGY CONVERSION"*
by: Bent Sørensen

227/92 "Computersimulering og fysik"
af: Per M.Hansen, Steffen Holm, Peter Maibom, Mads K. Dall Petersen, Pernille Postgaard, Thomas B.Schrøder, Ivar P. Zeck
Vejleder: Peder Voetmann Christiansen

228/92 "Teknologi og historie"
Fire artikler af:
Mogens Niss, Jens Høyrup, Ib Thiersen, Hans Hedal

229/92 "Masser af information uden betydning"
En diskussion af informationsteorien i Tor Nørretranders' "Mærk Verden" og en skitse til et alternativ basseret på andenordens kybernetik og semiotik.
af: Søren Brier

230/92 "Vinklens tredeling - et klassisk problem"
et matematisk projekt af
Karen Birkelund, Bjørn Christensen
Vejleder: Johnny Ottesen

231A/92 "Elektrondiffusion i silicium - en matematisk model"
af: Jesper Voetmann, Karen Birkelund, Mette Olufsen, Ole Møller Nielsen
Vejledere: Johnny Ottesen, H.B.Hansen

231B/92 "Elektrondiffusion i silicium - en matematisk model" Kildetekster
af: Jesper Voetmann, Karen Birkelund, Mette Olufsen, Ole Møller Nielsen
Vejledere: Johnny Ottesen, H.B.Hansen

232/92 "Undersøgelse om den simultane opdagelse af energiens bevarelse og især̃eles om de af Mayer, Colding, Joule og Helmholtz udførte arbejder"
af: L.Arleth, G.I.Dybkjær, M.T.Østergård
Vejleder: Dorthe Posselt

233/92 "The effect of age-dependent host mortality on the dynamics of an endemic disease and
Instability in an SIR-model with age-dependent susceptibility
by: Viggo Andreasen

234/92 "THE FUNCTIONAL DETERMINANT OF A FOUR-DIMENSIONAL BOUNDARY VALUE PROBLEM"
by: Thomas P. Branson and Peter B. Gilkey

235/92 OVERFLADESTRUKTUR OG POREUDVIKLING AF KOKS
- Modul 3 fysik projekt -
af: Thomas Jessen

236a/93 INTRODUKTION TIL KVANTE HALL EFFEKTEN

af: Anja Boisen, Peter Bøggild

Vejleder: Peder Voetmann Christiansen
Erland Brun Hansen

236b/93 STRØMSSAMMENBRUD AF KVANTE HALL EFFEKTEN

af: Anja Boisen, Peter Bøggild

Vejleder: Peder Voetmann Christiansen
Erland Brun Hansen

237/93 The Wedderburn principal theorem and Shukla cohomology

af: Lars Kadison

238/93 SEMIOTIK OG SYSTEMEGENSKABER (2)

Vektorbånd og tensorer

af: Peder Voetmann Christiansen

239/93 Valgsystemer - Modelbygning og analyse

Matematik 2. modul

af: Charlotte Gjerrild, Jane Hansen, Maria Hermannsson, Allan Jørgensen, Ragna Clauson-Kaas, Poul Lützen

Vejleder: Mogens Niss

240/93 Patologiske eksempler.
Om sære matematiske fisks betydning for den matematiske udvikling

af: Claus Dræby, Jørn Skov Hansen, Runa Ulsøe Johansen, Peter Meibom, Johannes Kristoffer Nielsen

Vejleder: Mogens Niss

241/93 FOTOVOLTAISK STATUSNOTAT 1

af: Bent Sørensen

242/93 Brovedligeholdelse - bevar mig vel

Analyse af Vejdirektoratets model for optimering af broreparationer

af: Linda Kyndlev, Kare Fundal, Kamma Tulinius, Ivar Zeck

Vejleder: Jesper Larsen

243/93 TANKEEKSPERIMENTER I FYSIKKEN

Et 1.modul fysikprojekt

af: Karen Birkelund, Stine Sofia Korremann

Vejleder: Dorthe Posselt

244/93 RADONTRANSFORMATIONEN og dens anvendelse i CT-scanning

Projektrapport

af: Trine Andreasen, Tine Guldager Christiansen, Nina Skov Hansen og Christine Iversen

Vejledere: Gestur Olafsson og Jesper Larsen

245a+b /93 Time-Of-Flight målinger på krystallinske halvledere
Specialerapport

af: Linda Szkotak Jensen og Lise Odgaard Gade

Vejledere: Petr Viscor og Niels Boye Olsen

246/93 HVERDAGSVIDEN OG MATEMATIK - LÆREPROCESSER I SKOLEN

af: Lena Lindenskov, Statens Humanistiske Forskningsråd, RUC, IMFUFA

247/93 UNIVERSAL LOW TEMPERATURE AC CONDUCTIVITY OF MACROSCOPICALLY DISORDERED NON-METALS

by: Jeppe C. Dyre

248/93 DIRAC OPERATORS AND MANIFOLDS WITH BOUNDARY

by: B. Booss-Bavnbek, K.P.Wojciechowski

249/93 Perspectives on Teichmüller and the Jahresbericht Addendum to Schappacher, Scholz, et al.

by: B. Booss-Bavnbek

With comments by W.Abikoff, L.Ahlfors, J.Cerf, P.J.Davis, W.Fuchs, F.P.Gardiner, J.Jost, J.-P.Kahane, R.Lohan, L.Lorch, J.Radkau and T.Söderqvist

250/93 EULER OG BOLZANO - MATEMATISK ANALYSE SET I ET VIDENSKABSTEORETISK PERSPEKTIV

Projektrapport af: Anja Juul, Lone Michelsen, Tomas Højgård Jensen

Vejleder: Stig Andur Pedersen

251/93 Genotypic Proportions in Hybrid Zones

by: Freddy Bugge Christiansen, Viggo Andreasen and Ebbe Thue Poulsen

252/93 MODELLERING AF TILFÆLDIGE FÆNOMENER

Projektrapport af: Birthe Friis, Lisbeth Helmgaard, Kristina Charlotte Jakobsen, Marina Mosbæk Johannessen, Lotte Ludvigsen, Mette Hass Nielsen

253/93 Kuglepakning

Teori og model

af: Lise Arleth, Kåre Fundal, Nils Kruse

Vejleder: Mogens Niss

254/93 Regressionsanalyse

Materiale til et statistikkursus

af: Jørgen Larsen

255/93 TID & BETINGET UAFHÆNGIGHED

af: Peter Harremoës

256/93 Determination of the Frequency Dependent Bulk Modulus of Liquids Using a Piezoelectric Spherical Shell (Preprint)

by: T. Christensen and N.B.Olsen

257/93 Modellering af dispersion i piezoelektriske keramikker

af: Pernille Postgaard, Jannik Rasmussen, Christina Specht, Mikko Østergård

Vejleder: Tage Christensen

258/93 Supplerende kursusmateriale til "Lineære strukturer fra algebra og analyse"

af: Mogens Brun Heefelt

259/93 STUDIES OF AC HOPPING CONDUCTION AT LOW TEMPERATURES

by: Jeppe C. Dyre

260/93 PARTITIONED MANIFOLDS AND INVARIANTS IN DIMENSIONS 2, 3, AND 4

by: B. Booss-Bavnbek, K.P.Wojciechowski

261/93 OPGAVESAMLING
Bredde-kursus i Fysik
Eksamensopgaver fra 1976-93

262/93 Separability and the Jones Polynomial
by: Lars Kadison

263/93 Supplerende kursusmateriale til "Lineære strukturer fra algebra og analyse" II
af: Mogens Brun Heefelt

264/93 FOTOVOLTAISK STATUSNOTAT 2
af: Bent Sørensen

265/94 SPHERICAL FUNCTIONS ON ORDERED SYMMETRIC SPACES
To Sigurdur Helgason on his sixtyfifth birthday
by: Jacques Faraut, Joachim Hilgert and Gestur Olafsson

266/94 Kommensurabilitets-oscillationer i laterale supergitre
Fysikspeciale af: Anja Boisen, Peter Bøggild, Karen Birkelund
Vejledere: Rafael Taboryski, Poul Erik Lindelof, Peder Voetmann Christiansen

267/94 Kom til kort med matematik på Eksperimentarium - Et forslag til en opstilling
af: Charlotte Gjerrild, Jane Hansen
Vejleder: Bernhelm Booss-Bavnbek

268/94 Life is like a sewer ...
Et projekt om modellering af aorta via en model for strømning i kloakrør
af: Anders Marcussen, Anne C. Nilsson, Lone Michelsen, Per M. Hansen
Vejleder: Jesper Larsen

269/94 Dimensionsanalyse en introduktion
metaprojekt, fysik
af: Tine Guldager Christiansen, Ken Andersen, Nikolaj Hermann, Jannik Rasmussen
Vejleder: Jens Højgaard Jensen

270/94 THE IMAGE OF THE ENVELOPING ALGEBRA AND IRREDUCIBILITY OF INDUCED REPRESENTATIONS OF EXPONENTIAL LIE GROUPS
by: Jacob Jacobsen

271/94 Matematikken i Fysikken.
Opdaget eller opfundet
NAT-BAS-projekt
vejleder: Jens Højgaard Jensen

272/94 Tradition og fornyelse
Det praktiske elevarbejde i gymnasiets fysikundervisning, 1907-1988
af: Kristian Hoppe og Jeppe Guldager
Vejledning: Karin Beyer og Nils Hybel

273/94 Model for kort- og mellemdistanceløb
Verifikation af model
af: Lise Fabricius Christensen, Helle Pilemann, Bettina Sørensen
Vejleder: Mette Olufsen

274/94 MODEL 10 - en matematisk model af intravenøse anæstetikas farmakokinetik
3. modul matematik, forår 1994
af: Trine Andreasen, Bjørn Christensen, Christine Green, Anja Skjoldborg Hansen. Lisbeth Helmgaard
Vejledere: Viggo Andreasen & Jesper Larsen

275/94 Perspectives on Teichmüller and the Jahresbericht
2nd Edition
by: Bernhelm Booss-Bavnbek

276/94 Dispersionsmodellering
Projektrapport 1. modul
af: Gitte Andersen, Rehannah Borup, Lisbeth Friis, Per Gregersen, Kristina Vejrø
Vejleder: Bernhelm Booss-Bavnbek

277/94 PROJEKTARBEJDSPÆDAGOGIK - Om tre tolkninger af problemorienteret projektarbejde
af: Claus Flensted Behrens, Frederik Voetmann Christiansen, Jørn Skov Hansen, Thomas Thingstrup
Vejleder: Jens Højgaard Jensen

278/94 The Models Underlying the Anaesthesia Simulator Sophus
by: Mette Olufsen(Math-Tech), Finn Nielsen (RISØ National Laboratory), Per Føge Jensen (Herlev University Hospital), Stig Andur Pedersen (Roskilde University)

279/94 Description of a method of measuring the shear modulus of supercooled liquids and a comparison of their thermal and mechanical response functions.
af: Tage Christensen

280/94 A Course in Projective Geometry
by Lars Kadison and Matthias T. Kromann

281/94 Modellering af Det Cardiovaskulære System med Neural Pulskontrol
Projektrapport udarbejdet af:
Stefan Frello, Runa Ulsøe Johansen, Michael Poul Curt Hansen, Klaus Dahl Jensen
Vejleder: Viggo Andreasen

282/94 Parallelle algoritmer
af: Erwin Dan Nielsen, Jan Danielsen, Niels Bo Johansen

283/94 Grænser for tilfældighed
(en kaotisk talgenerator)

af: Erwin Dan Nielsen og Niels Bo Johansen

284/94 Det er ikke til at se det, hvis man ikke lige ve' det!
Gymnasiematematikkens begrundelsesproblem

En specialerapport af Peter Hauge Jensen
og Linda Kyndlev

Vejleder: Mogens Niss

285/94 Slow coevolution of a viral pathogen and its diploid host

by: Viggo Andreasen and
Freddy B. Christiansen

286/94 The energy master equation: A low-temperature approximation to Bässler's random walk model

by: Jeppe C. Dyre

287/94 A Statistical Mechanical Approximation for the Calculation of Time Auto-Correlation Functions

by: Jeppe C. Dyre

288/95 PROGRESS IN WIND ENERGY UTILIZATION

by: Bent Sørensen

289/95 Universal Time-Dependence of the Mean-Square Displacement in Extremely Rugged Energy Landscapes with Equal Minima

by: Jeppe C. Dyre and Jacob Jacobsen

290/95 Modellering af uregelmæssige bølger
Et 3.modul matematik projekt
af: Anders Marcussen, Anne Charlotte Nilsson, Lone Michelsen, Per Mørkegaard Hansen
Vejleder: Jesper Larsen

291/95 1st Annual Report from the project
LIFE-CYCLE ANALYSIS OF THE TOTAL DANISH ENERGY SYSTEM
an example of using methods developed for the OECD/IEA and the US/EU fuel cycle externality study
by: Bent Sørensen

292/95 Fotovoltaisk Statusnotat 3
af: Bent Sørensen

293/95 Geometridiskussionen - hvor blev den af?
af: Lotte Ludvigsen & Jens Frandsen
Vejleder: Anders Madsen

294/95 Universets udvidelse -
et metaprojekt
Af: Jesper Duelund og Birthe Friis
Vejleder: Ib Lundgaard Rasmussen

295/95 A Review of Mathematical Modeling of the Controled Cardiovascular System
By: Johnny T. Ottesen

296/95 RETIKULER den klassiske mekanik
af: Peder Voetmann Christiansen

297/95 A fluid-dynamical model of the aorta with bifurcations

by: Mette Olufsen and Johnny Ottesen

298/95 Mordet på Schrödingers kat - et metaprojekt om to fortolkninger af kvantemekanikken

af: Maria Hermannsson, Sebastian Horst, Christina Specht

Vejledere: Jeppe Dyre og Peder Voetmann Christiansen

299/95 ADAM under figenbladet - et kig på en samfundsvidenskabelig matematisk model

Et matematisk modelprojekt
af: Claus Dræby, Michael Hansen, Tomas Højgård Jensen
Vejleder: Jørgen Larsen

300/95 Scenarios for Greenhouse Warming Mitigation

by: Bent Sørensen

301/95 TOK Modellering af træers vækst under påvirkning af ozon

af: Glenn Møller-Holst, Marina Johannessen, Birthe Nielsen og Bettina Sørensen

Vejleder: Jesper Larsen

302/95 KOMPRESSORER - Analyse af en matematisk model for aksialkompressorer

Projektrapport af: Stine Bøggild, Jakob Hilmer, Pernille Postgaard

Vejleder: Viggo Andreasen

303/95 Masterlignings-modeller af Glasovergangen
Termisk-Mekanisk Relaksation
Specialerapport udarbejdet af:

Johannes K. Nielsen, Klaus Dahl Jensen

Vejledere: Jeppe C. Dyre, Jørgen Larsen

304a/95 STATISTIKNOTER Simple binomialfordelingsmodeller
af: Jørgen Larsen

304b/95 STATISTIKNOTER Simple normalfordelingsmodeller
af: Jørgen Larsen

304c/95 STATISTIKNOTER Simple Poissonfordelingsmodeller
af: Jørgen Larsen

304d/95 STATISTIKNOTER Simple multinomialfordelingsmodeller
af: Jørgen Larsen

304e/95 STATISTIKNOTER Mindre matematisk-statistisk opslagsværk indeholdende bl.a. ordforklaringer, resuméer og tabeller
af: Jørgen Larsen

305/95 The Maslov Index:
A Functional Analytical Definition
And The Spectral Flow Formula

By: B. Booss-Bavnbek, K. Furutani

306/95 Goals of mathematics teaching

Preprint of a chapter for the forth-comming International Handbook of Mathematics Education (Alan J.Bishop, ed)

By: Mogens Niss

307/95 Habit Formation and the Thirdness of Signs

Presented at the semiotic symposium

The Emergence of Codes and Intensions as a Basis of Sign Processes

By: Peder Voetmann Christiansen

308/95 Metaforer i Fysikken

af: Marianne Wilcken Bjerregaard, Frederik Voetmann Christiansen, Jørn Skov Hansen, Klaus Dahl Jensen Ole Schmidt

Vejledere: Peder Voetmann Christiansen og Petr Viscor

309/95 Tiden og Tanken
En undersøgelse af begrebsverdenen Matematik udført ved hjælp af en analogi med tid

af: Anita Stark og Randi Petersen

Vejleder: Bernhelm Booss-Bavnbek

310/96 Kursusmateriale til "Lineære strukturer fra algebra og analyse" (E1)

af: Mogens Brun Heefelt

311/96 2nd Annual Report from the project
LIFE-CYCLE ANALYSIS OF THE TOTAL DANISH ENERGY SYSTEM

by: Hélène Connor-Lajambe, Bernd Kuemmel, Stefan Krüger Nielsen, Bent Sørensen

312/96 Grassmannian and Chiral Anomaly

by: B. Booss-Bavnbek, K.P.Wojciechowski